APPLICATION OF PHOTODYNAMIC THERAPY WITH MAGNETIC FIELDS AND DYES FOR THE TREATMENT OF MICROBIAL SKIN INFECTIONS IN VITRO AND IN VIVO

ALI ADIL TURKI AL-DALAWI

UNIVERSITI SAINS MALAYSIA

2024

APPLICATION OF PHOTODYNAMIC THERAPY WITH MAGNETIC FIELDS AND DYES FOR THE TREATMENT OF MICROBIAL SKIN INFECTIONS IN VITRO AND IN VIVO

by

ALI ADIL TURKI AL-DALAWI

Thesis submitted in fulfillment of the requirements for the degree of Doctor of Philosophy

March 2024

Dedication

This work is dedicated to the



HIS FAMILY AND COMPANIONS

ACKNOWLEDGEMENT

"In the name of Allah, the Most Gracious, the Most Merciful"

I endured easy and difficult, good and thought-provoking times in the course of this

research; hence I would like to thank Allah Almighty for His mercy, and bounty and

for granting me health, patience, and the willpower to satisfactorily carry out this

research. I would like to express my sincere gratitude and appreciation to my main

supervisor, Professor. Dr. Nursakinah Binti Suardi, and co-supervisors, Assoc. Prof.

Dr. Mahdi Ali Sukkar Al-Faraaon and Prof. Dr. Naser Mahmoud Ahmed for their

expert guidance, valuable assistance, motivation, and immense knowledge towards

the realization of this study. I would also like to acknowledge generally, Universiti

Sains Malaysia (USM), and the academic and non-academic staff of the School of

Physics, USM for their assistance and support of this research. I would also like to

express my gratitude and appreciation to Al-Qadisiyah University and Al-Qasim

Green University in Iraq, for their unlimited support in the realization of this study. I

would like to extend my sincere appreciation and gratitude to the many friends and

colleagues who helped make this work possible. I would also like to dedicate my

deep appreciation to my parents, sisters, and brother for their love, support, patience,

and faith in me. Last but not least, I dedicate my love and gratitude to my wife

(Amal) and children (Élan, Anya). All my accomplishments would not be possible

without them in my life. I repeat, will not forget the contributions and stances of my

supervisor, Dr. Nursakinah Suardi, for her kind interests.

Ali A. Aldalawi

2024

Penang, Malaysia

ii

TABLE OF CONTENTS

ACK	NOWL	EDGEMENT	ii
TAB	LE OF	CONTENTS	iii
LIST	OF TA	BLES	X
LIST	OF FIG	GURES	xiii
LIST	OF SY	MBOLS	xix
LIST	OF AB	BREVIATIONS	xxi
LIST	OF AP	PENDICES	xxiii
ABS	ΓRAK		xxiv
ABS	ГRАСТ		xxvi
СНА	PTER 1	INTRODUCTION	1
1.1	Backg	round of the Study	1
1.2	Proble	em Statement	3
1.3	Resea	rch Objectives	4
1.4	Origin	ality of the Study	5
1.5	Scope	of the Study	5
1.6	Outlin	e of Thesis	7
СНА	PTER 2	LITERATURE REVIEW AND THEORETICAL BACKGROUND	8
2.1	Introd	uction	8
2.2	Photo	dynamic therapy (PDT)	8
2.3	Putati	ve mechanisms of action of PDT	10
2.4	Putati	ve mechanisms of action of aPDT	12
2.5	PDT (Components	13
	2.5.1	Photosensitizers	13
	2.5.2	Toluidine blue dye (TB)-Induced Protoporphyrin IX (PPIX)	15
		2.5.2(a) Natural chlorophylls	15

	2.5.3	Light source, transport, and delivery	16
	2.5.4	Tissue oxygen	17
2.6	Tissue	e regeneration and wound-healing	18
2.7	Light	Technology for Topical PDT	19
	2.7.1	Light interaction with biological tissue	19
		2.7.1(a) Absorption	20
		2.7.1(b) Reflection	21
		2.7.1(c) Refraction	22
		2.7.1(d) Scattering	23
	2.7.2	Putative mechanisms of action of aPDT upon absorption	23
		2.7.2(a) Photochemical	23
		2.7.2(b) Photophysical	24
	2.7.3	Basics on dosimetry and beam	25
2.8	Clinic	al and Preclinical Studies of aPDT	26
2.9	Light	Source	28
	2.9.1	Lasers	28
		2.9.1(a) Diode lasers	29
2.10	Beam	Profiles and Depth of Penetration	30
	2.10.1	Light transmission techniques for PDT in tissue	30
	2.10.2	Laser depth of penetration	31
	2.10.3	Light distribution during laser irradiation of tissue	31
2.11	Putati	ve mechanisms of laser action	33
2.12	Magne	etic Fields (MFs)	34
	2.12.1	Static magnetic fields	35
	2.12.2	Magnetic fields and wound repair: Mechanism of action	37
	2.12.3	Antimicrobial magnetic fields	38
2.13	Overv	riew of Studies	39

CHA	PTER 3	MATE	RIALS AND METHODOLOGY	42
3.1	Introd	uction		42
3.2	Instru	mentation,	Materials, and Equipment	42
	3.2.1	Single-Mo	ode Diode Laser	42
	3.2.2	Omega D	iode Laser	43
	3.2.3	Laser Pov	ver Meter Instrument	44
	3.2.4	Magnetic	Flux Density Meter (MFDM) Instrument	45
	3.2.5	Instrumen	ts Used in Preparing Optical Pigments	46
		3.2.5(a)	Analytical Balance and Magnetic Stirrer	46
		3.2.5(b)	Micro Hematocrit Centrifuge	46
		3.2.5(c)	Multifunctional Instrument pH Meter	47
		3.2.5(d)	UV-Vis Spectrophotometer	47
		3.2.5(e)	Fourier Transform Infrared (FTIR) Spectrometer	48
		3.2.5(f)	Fluorescence Spectrometer	49
		3.2.5(g)	Drying Oven	49
		3.2.5(h)	Distillation Device	50
	3.2.6	Instrumen	tations used in the Preparation of Bacterial Cultures	50
		3.2.6(a)	Laminar Flow Hood (LFH)	50
		3.2.6(b)	Bacterial Incubator	50
		3.2.6(c)	Autoclave	51
		3.2.6(d)	Vortex Mixer	51
	3.2.7		tations used in the (Characterization of Histological es)	51
		3.2.7(a)	Microtome	51
		3.2.7(b)	Electron Microscopy	52
	3.2.8	Equipmen	nt used in Therapeutic Settings	52
		3.2.8(a)	Magnetic Field	52
		3.2.8(b)	Preparation Box for Experimental Setup	54

	3.2.9	Chemical	Materials used in this Study	55
		3.2.9(a)	Ethanol	56
		3.2.9(b)	Toluidine Blue (TB)	56
		3.2.9(c)	Sodium Chloride	57
		3.2.9(d)	Formalin Solution (Formaldehyde)	57
		3.2.9(e)	Ketamine and Xylazine	58
	3.2.10	Culture M	edia	58
3.3	Metho	odology		59
	3.3.1	Study Des	ign	59
		3.3.1(a)	Characterization of PS pigments	60
	3.3.2	MRSA Ina	activation (In Vitro)	61
		3.3.2(a)	In vitro sample acquisition and preparation	61
		3.3.2(b)	Photosensitizer chemical preparation – Toluidine blue dye	62
		3.3.2(c)	Bacterial Preparation	63
			3.3.2(c)(i) Identification of Bacterial Isolation	63
			3.3.2(c)(ii) Preparation of a standardized inoculum from a bacterial culture	65
		3.3.2(d)	Measurement of Magnetic Flux Density	65
		3.3.2(e)	Pre-irradiation Procedure	67
		3.3.2(f)	Irradiation Procedure	68
		3.3.2(g)	Light Transmission Measurement	72
		3.3.2(h)	Bacterial Colony Counts	73
	3.3.3	MRSA Vi	ability (In Vivo)	75
		3.3.3(a)	Animal Model	75
		3.3.3(b)	Plant-based photosensitizer preparation	76
			3.3.3(b)(i) Characterization of photosensitizers (PS)	78
		3.3.3(c)	Pre-irradiation procedure	80

			3.3.3(c)(i) Wound creation	80
			3.3.3(c)(ii) Implantation of bacteria	81
		3.3.3(d)	Irradiation procedure	82
		3.3.3(e)	Bacterial colony counts	83
		3.3.3(f)	Tissue biopsy	85
	3.3.4	Histologic	al Evaluation	85
	3.3.5	Calibration	of Laser	86
	3.3.6	Ethical Cle	earance	87
	3.3.7	Statistical	Analysis	87
CHA	PTER 4	RESULTS	S AND DISCUSSION	89
4.1	Introd	uction		89
4.2	Light '	Transmissio	n Measurement In Vitro	89
4.3 Characterization of Photosensitizers (Pigments)		of Photosensitizers (Pigments)	95	
	4.3.1	PH test of	natural PS	95
	4.3.2	Electrical (Conductivity	97
	4.3.3	Density		98
	4.3.4	UV–Visib	le Spectroscopy Analysis	100
	4.3.5	FTIR Anal	lysis	104
	4.3.6	Fluorescen	nt Analysis	106
4.4	MRSA	A Inactivation	on (In-Vitro)	108
	4.4.1	Laser grou	ıps	108
		4.4.1(a)	The in vitro MRSA susceptibility to light absorption at different wavelengths and treatment efficacy patterns	110
	4.4.2	Laser with	PS groups	112
		4.4.2(a)	Concordance of the in vitro anti-MRSA effect by aPDT, but with varying survival patterns depending on the efficiency of the treatment	115
	112	I ocon with	depending on the efficacy of the treatment	115
	441	Laser with	HIMPHEL VIOLIDS	

		4.4.3(a)	The in vitro anti-MRSA effect is consistent with varied survival patterns using laser and external MFs stimulation	. 119
	4.4.4	Laser with	(PS and magnet) groups	. 121
		4.4.4(a)	The in vitro anti-MRSA effect is consistent with varied survival patterns using aPDT in conjunction with external MFs stimulation	. 124
4.5	MRSA	Viability (In Vivo)	. 125
	4.5.1	Effect of 5	30 nm laser treatment on MRSA viability	. 125
		4.5.1(a)	Laser groups	. 125
		4.5.1(b)	Laser with magnet groups	. 126
		4.5.1(c)	Laser with PS groups	. 127
		4.5.1(d)	Laser with (PS and magnet) groups	. 128
	4.5.2	Effect of 6	60 nm laser treatment on MRSA viability	. 129
		4.5.2(a)	Laser groups	. 129
		4.5.2(b)	Laser with magnet groups	. 130
		4.5.2(c)	Laser with PS groups	. 131
		4.5.2(d)	Laser with (PS and magnet) groups	. 132
	4.5.3		vo anti-MRSA effect is consistent with diverse atterns using laser stimulation at 530 nm and 660 nm	. 133
	4.5.4	survival pa	vo anti-MRSA effect is consistent with diverse atterns using laser stimulation at 530 nm and 660 nm tion with external MFs	. 135
	4.5.5	with varying	ce of the in vivo anti-MRSA effect by aPDT, but ng survival patterns depending on the efficacy of the	. 137
	4.5.6	conjunction	lity of the in vivo anti-MRSA effect by aPDT in n with external MFs, but with varying survival pending on the efficacy of the treatment	. 139
4.6	Histol	ogical Evalu	nation	. 141
	4.6.1	Blank grou	ip (no treatment)	. 142
	4.6.2	Control gra	oups	. 142

	4.6.3	Treatment	groups	144
		4.6.3(a)	Laser groups	144
		4.6.3(b)	Laser with PS groups	146
		4.6.3(c)	Laser with magnet groups	148
		4.6.3(d)	Laser with (PS and magnet) groups	150
4.7	Therap	eutic Evalu	ation	154
	4.7.1	Control gro	oups	154
	4.7.2	Laser treat	ment	155
	4.7.3	Laser with	PS treatment	156
	4.7.4	Laser with	a magnet treatment	156
	4.7.5	Laser with	PS and a magnet treatment	157
	4.7.6	Evaluating	the impact of various treatments	158
CHAP	PTER 5	CONCLU	SION AND FUTURE RECOMMENDATIONS	161
5.1	Conclu	ısions		161
5.2	Recom	nmendations	for future research	162
5.3	Limita	tions of the	study	163
REFE	RENC	ES		164
APPE	NDICE	ES		
LIST	LIST OF PURLICATIONS			

LIST OF TABLES

		Page
Table 2.1	Wavelength and approximate penetration depth in tissues (Ash et al., 2017; Lanzafame, 2020)	28
Table 2.2	Summary table of comparison of the literature review of PDT parameters with/without the use of magnetic stimulation in the treatment of different disease conditions (Kumar & Girija, 2022; Martins et al., 2021)	41
Table 3.1	Chemical materials	55
Table 3.2	Type of media used	59
Table 3.3	The estimated magnetic flux density difference between the two sides of the sample	67
Table 3.4	Formulation of nutritional supplements for rats during the therapeutic phase, supplemented by multivitamins, minerals, and amino acids (Cho Livet- AM, 10g/ kg) (Turner et al., 2011).	76
Table 3.5	UV-Vis Spectroscopy Analysis of Dye Samples	78
Table 4.1	Differences in the penetration depths of 660nm (red) and 532nm (green) laser light through varying thicknesses of beef tissue	92
Table 4.2	Differences in the penetration depths of 660nm (red) and 532nm (green) laser light through varying thicknesses of chicken breast tissue	93
Table 4.3	pH values for natural PS corresponding to different extraction durations, spanning from 4 hours to 24 hours	96
Table 4.4	Electrical conductivity for plant photoactive dyes for aPDT within the range of 100 to 1000 $\mu S/cm$	98
Table 4.5	Density values for natural PS	99
Table 4.6	The bonds wave number of chlorophyll pigments from chard for 24 hours	105
Table 4.7	The bonds wave number of chlorophyll pigments from spinach during 24 hours	105
Table 4.8	Multiple comparisons of laser effect between/within groups treated across various thicknesses of beef tissue	108

Table 4.9	Multiple comparisons of laser effect between/within groups treated across various thicknesses of chicken breast tissue
Table 4.10	Multiple comparisons of laser effect with PS between/within groups treated across various thicknesses of beef tissue
Table 4.11	Multiple comparisons of laser effect with PS between/within groups treated across various thicknesses of chicken breast tissue
Table 4.12	Multiple comparisons of laser effect with magnet between/within groups treated across various thicknesses of beef tissue
Table 4.13	Multiple comparisons of laser effect with magnet between/within groups treated across various thicknesses of chicken breast tissue
Table 4.14	Multiple comparisons of laser effect with magnet and PS between/within groups treated across various thicknesses of beef tissue
Table 4.15	Multiple comparisons of laser effect with magnet and PS between/within groups treated across various thicknesses of chicken breast tissue
Table 4.16	Mean percentage of MRSA viability with a standard deviation function in rats after 530 nm laser treatment over four consecutive days
Table 4.17	Mean percentage of MRSA viability with a standard deviation function in rats after treatment at 530 nm laser with a magnet over four consecutive days
Table 4.18	Mean percentage of MRSA viability with a standard deviation function in rats after treatment at 530 nm laser with dyes over four consecutive days
Table 4.19	Mean percentage of MRSA viability with a standard deviation function in rats after treatment at 530 nm laser with dyes and a magnet over four consecutive days
Table 4.20	Mean percentage of MRSA viability with a standard deviation function in rats after 660 nm laser treatment over four consecutive days
Table 4.21	Mean percentage of MRSA viability with a standard deviation function in rats after treatment at 660 nm laser with a magnet over four consecutive days

Table 4.22	Mean percentage of MRSA viability with a standard deviation function in rats after treatment at 660 nm laser			
	with dyes over four consecutive days	131		
Table 4.23	Mean percentage of MRSA viability with a standard deviation function in rats after treatment at 660 nm laser with dyes and a magnet over four consecutive days	132		

LIST OF FIGURES

		Page
Figure 2.1	A typical scheme of the mechanism of action of PDT (Zhu & Finlay, 2008)	11
Figure 2.2	Scheme of the mechanism of activation of aPDT (Carrera et al., 2016)	13
Figure 2.3	Interactions between light and tissue (Plaetzer et al., 2009)	20
Figure 3.1	Single-mode diode laser (532 & 660nm)	43
Figure 3.2	Omega diode laser	44
Figure 3.3	Laser power meter	45
Figure 3.4	Magnetic flux density meter (MFDM)	46
Figure 3.5	Neodymium magnets used in the experiment (Munaz et al., 2013)	53
Figure 3.6	Preparation of the experimental setup involves the following components: (a) Arranging a movable wooden platform within the box to accommodate the samples (b) Establishing the placement of barriers around the samples (c) Installing the lens for the laser power meter (d) Identifying the specific location for the tissue samples (e) Positioning external MFs around the samples (f) Implementing a vertical irradiation mechanism	55
Figure 3.7	Flow chart of study designed for this research	60
Figure 3.8	Flow chart showing the characterization of PS pigments	61
Figure 3.9	Mechanism of irradiating chicken breast and beef tissue samples inside a closed box	69
Figure 3.10	The mechanism of laser irradiation involved the following steps: (a) positioning the external MFs around the tissue samples (b) aligning the platform to direct the laser beam vertically to the middle of the sample (c and d) performing laser irradiation at both 532 nm and 650 nm wavelengths	70
Figure 3.11	(a) Preparation of samples (b) Setup of the experimental platform (c) Calibration of magnets (d) Positioning of magnets around the sample before dye placement	72

Figure 3.12	Method for in vitro tissue light transmission measurement: (a) Tissue thickness preparation (b) Calibration for thickness measurement accuracy (c) Placement of an LP1 lens beneath the sample (d) Alignment of the light spot to the middle of the sample
Figure 3.13	Extract PS from various plant leaves over different time intervals ranging from 4 to 24 hours
Figure 3.14	Creation of wounds in rats
Figure 3.15	The mechanism of laser irradiation of rats involves two main components: (a) positioning the laser lens in proximity to the lesion site above the midline and (b) placing a magnet between the two sides of the lesioned specimen to ensure that the laser spot is precisely centered
Figure 4.1	The transmittance of laser light from the first moments at 660 nm and 532 nm across various thicknesses of beef tissue
Figure 4.2	The maximum transmittance of laser light at 660 nm and 532 nm across various thicknesses of beef tissue for more than 10 consecutive minutes
Figure 4.3	The transmittance of laser light from the first moments at 660 nm and 532 nm across various thicknesses of chicken breast tissue
Figure 4.4	The maximum transmittance of laser light at 660 nm and 532 nm across various thicknesses of chicken breast tissue for more than 10 consecutive minutes
Figure 4.5	Absorption spectra of PS according to the period prepared for their extraction. (a) Presents the absorption spectrum of chlorophyll pigment isolated from chard over 24 hours, (b) Presents the absorption spectrum of chlorophyll pigment isolated from chard over 20 hours, (c) Presents the absorption spectrum of chlorophyll pigment isolated from spinach over 24 hours, (d) Presents the absorption spectrum of chlorophyll pigment isolated from spinach over 16 hours 102
Figure 4.6	Absorption spectra of PS according to the period prepared for their extraction. (a) The absorption spectrum of isolated hibiscus pigment over 24 hours, (b) The absorption spectrum of isolated carrots pigment over 20 hours, (c) The absorption spectrum of isolated tangerine pigment over 24 hours
Figure 4.7	FTIR spectra of chlorophyll extracted chard during 24 hours

Figure 4.8	FTIR spectra of chlorophyll extracted spinach during 24 hours	105
Figure 4.9	(a) Fluorescence spectra obtained from chard dye extracted over a 24-hour, (b) Fluorescence spectra acquired from chard dye extracted over a 20-hour, (c) Fluorescence spectra derived from spinach dye extracted over 24 hours, (d) Fluorescence spectra resulting from spinach dye extraction over a 12-hour, and (e) Fluorescence spectra recorded from hibiscus dye extracted over 24 hours.	107
Figure 4.10	The percentage of MRSA viability after irradiation with wavelengths of 660 nm and 532 nm for various beef tissue thicknesses	109
Figure 4.11	The percentage of MRSA viability after irradiation with wavelengths of 660 nm and 532 nm for various chicken tissue thicknesses	110
Figure 4.12	The percentage of MRSA viability after irradiation with wavelengths of 660 nm and 532 nm with PS for various beef tissue thicknesses	113
Figure 4.13	The percentage of MRSA viability after irradiation with wavelengths of 660 nm and 532 nm with PS for various chicken tissue thicknesses	115
Figure 4.14	The percentage of MRSA viability after irradiation with wavelengths of 660 nm and 532 nm with magnet-assisted for various beef tissue thicknesses	117
Figure 4.15	The percentage of MRSA viability after irradiation with wavelengths of 660 nm and 532 nm with magnet-assisted for various chicken tissue thicknesses	119
Figure 4.16	The percentage of MRSA viability after irradiation with wavelengths of 660 nm and 532 nm with PS and magnet for various beef tissue thicknesses	122
Figure 4.17	The percentage of MRSA viability after irradiation with wavelengths of 660 nm and 532 nm with PS and magnet for various chicken tissue thicknesses	123
Figure 4.18	Percentage of MRSA viability in rats after 532 nm laser treatment over four consecutive days	126
Figure 4.19	Percentage of MRSA viability in rats after treatment at 532 nm laser with a magnet over four consecutive days	127
Figure 4.20	Percentage of MRSA viability in rats after treatment at 532 nm laser with dyes over four consecutive days	128

Figure 4.21	Percentage of MRSA viability in rats after treatment at 532 nm laser with dyes and a magnet over four consecutive days 129
Figure 4.22	Percentage of MRSA viability in rats after 660 nm laser treatment over four consecutive days
Figure 4.23	Percentage of MRSA viability in rats after treatment at 660 nm laser with a magnet over four consecutive days
Figure 4.24	Percentage of MRSA viability in rats after treatment at 660 nm laser with dyes over four consecutive days
Figure 4.25	Percentage of MRSA viability in rats after treatment at 660 nm laser with dyes and a magnet over four consecutive days 133
Figure 4.26	Histological section taken from a blank, uninfected sample 142
Figure 4.27	(a) A view at the wound site of the control group on the first day reveals a defect area with inflammatory cells (indicated by the head arrow). (b) Upon closer examination of the previous image (a) from day one in the control group, a magnified view depicts a defect area and an accumulation of inflammatory cells (head arrow). (c) Further magnification of the previous image (b) View of day one in the control group shows a defect of area and accumulation of inflammatory cells (head arrow)
Figure 4.28	(a) The microphotograph depicting the wound site after a 4-day duration in the control group reveals granulation tissue at the defect area, migrating epithelial cells (head arrow), fat cells, granulation tissue (GT), collagen fibers (arrow), and a new blood vessel (BV). (b) Magnification of the previous picture (a), the microphotograph taken after 4 days of the control application illustrates migrating epithelial cells at the wound area (head arrow), collagen fibers (arrow), fibroblasts (FB), and a blood vessel (BV)
Figure 4.29	(a) Microphotograph of wound site after 1 day reveals a defect area with a sparse presence of inflammatory cells (arrow). (b) Enlargement of the previous image (a) A 1-day magnified view shows a limited number of inflammatory cells (arrow) and fibroblasts (FB).
Figure 4.30	(a) Microphotograph after 4 days of treatment, shows migrating epithelial cells at the defect of edge (DA), and the presence of a new collagen fiber (arrow). (b) Magnification of the previous picture (a) microphotograph after 4 days of application, shows epithelial cells at the defect of edge (head arrow), Collagen fiber (arrow), and Fibroblast (FB)

Figure 4.31	(a) View on the first-day image shows collagen fibers (arrow), epithelial cells (head arrow), and the presence of fibroblast (FB). (b) Magnification of the previous picture (a) A Close examination of day 1 reveals a magnified view showing collagen fibers (arrow), epithelial cells (head arrow), and the presence of fibroblasts (FB)
Figure 4.32	 (a) Microphotograph after 4 days of treatment shows defect area, complete epithelialization at the defect of edge, collagen fiber (arrow), fibroblast (FB), and fat cells (FC). (b) Magnification of the previous picture (a) microphotograph after 4 days of the application shows complete epithelialization at the defect of edge (head arrow), collagen fiber (arrow), and fibroblast (FB).
Figure 4.33	(a) In the microphotograph of the wound site on the 1-day, granulation tissue is evident at the defect area (GT), accompanied by migrating epithelial cells (head arrow) and the presence of collagen fibers (arrow). (b) Enlargement of the previous photomicrograph (a) the damaged area reveals clear migration of the epithelium and epithelial cells (head arrow), along with the presence of collagen fibers (arrow) and fibroblasts (FB).
Figure 4.34	(a) Microphotograph of wound site of 4-days duration shows a defect of area, migrating epithelial cells (arrowhead), fibroblast (FB), collagen fiber (arrow), and new blood vessels (BV). (b) Enlargement of the previous photomicrograph (a) shows the emergence of new blood vessels (BV), fibroblasts (FB), epithelial cells (head arrow), and collagen fibers (arrow).
Figure 4.35	(a) Microphotograph of wound site of combination treatment 1-day duration shows complete epithelialization at the edge of the defect (head arrow), fibroblast (FB), and new blood vessels (BV) collagen fiber (arrow). (b) Magnification of the previous Figure (a) microphotograph after 1-day of combination treatment shows complete epithelialization at the edge of the defect (head arrow), and the presence of collagen fiber (arrow)
Figure 4.36	(a) Microphotograph after 4 days of combination treatment shows complete epithelialization at the defect of edge, fat cells (FC), hair follicles (head arrow), and collagen fiber (arrow), (b) Magnification of previous picture (a) microphotograph after 4 days of combination treatment shows complete epithelialization at the defect of edge (head arrow), collagen fiber (arrow), and fibroblast (FB)

Figure 4.37	Microphotographs depicting the combination treatment display the changes observed between day 1 and day 4 after irradiation. The image highlights the entire epithelium at the edge of the defect, fat cells (FC), hair follicles (indicated by a vertical arrow), collagen fibers (arrow), and fibroblasts (FB).
Figure 4.38	Control group models during the bacterial infection stage
Figure 4.39	(a) Effects of a single day's laser treatment on a particular specimen, where the wound site showed little inflammation, characterized by redness surrounding the injury, (b) the wound site 3 days after treatment shows thin epithelium (0.5 cm) and diminished redness around the periphery of the lesion, (c) shows a modest improvement in wound healing four days after treatment, showcasing transparent epiphysis with minimal skin redness
Figure 4.40	(a) Effects of laser treatment with the PS for three days. One of the selected specimens demonstrated superior healing, characterized by a wound border of about 0.8 cm, free of significant swelling around the periphery of the lesion, in addition to dense epithelialization, and normal mobility, (b) the wound site shows more favorable improvement, characterized by decreased swelling after the fourth day of treatment. Acceptable healing was observed at the site of injury, measuring approximately 0.7 cm, with reepithelialization beginning
Figure 4.41	Sample exposed to laser with magnet for four days
Figure 4.42	The samples (a & b) that were exposed to aPDT in conjunction with the external MFs for two days, (c & d) the two final samples, both of which underwent treatment for four consecutive days
	· · · · · · · · · · · · · · · · · · ·

LIST OF SYMBOLS

°C Degree Celsius

μl Microliter

 μ m Micrometer (1×10⁻⁶ m)

μW Microwatts

¹O₂ Singlet Oxygen

¹PS Low Energy Level

¹PS* Excited Singlet State

³O₂ Ground-State Molecular Oxygen

A Area

Al Aluminum

B Constant

C Speed of light

d Tissue thickness modifier

E Energy density

Eg Band gap energy

eV Electron volte

h Plank's constant

hv Photon energy

I Intensity

I Light transmission intensity at the surface of the tissue

The incident intensity of light into tissues, and takes values between I_0

0 and 1, 2, 3....etc.

J Joules

k Boltzmanconstant

ml Milliliters

mW Milliwatts

nm Nanometer $(1 \times 10^{-9} \text{ m})$

O₂ Transfer Energy

P Power

P_{in} Power intensity

r² Radius square

S₀ Ground State

S₁ Excited State

T Light transmittance

T Time

T₁ Excited Tertiary State

us Microsiemens

W Power

W Watt, Conversion readings

wi% Relative intensity

wt% Weight percentage

γ Factor

 λ Wavelength

 π Fixed ratio

ν Photon's frequency

LIST OF ABBREVIATIONS

aPDT Antimicrobial Photodynamic Therapy

ATP Adenosine Triphosphate

BV Blood vessel

CFU Colony-Forming Unit

CTM Conventional Tissue Models

CW Continuous wave

DA Defect area

df Degrees of freedom

ECM Electronic control module

ED Energy density

FB Fibroblast

FC Fat cells

FT-IR Fourier Transform Infrared

GaAlAs Gallium Aluminum arsenide diode laser

GN Bacteria gram-negative

GP⁺ Bacteria gram-positive

GT Granulation tissue

HPD Hematoporphyrin Derivatives

IRDM Infrared Data Manager

K Ketamine

LFH Laminar Flow Hood

LLLT Low-Level Laser Therapy

LP1 Laser Power Meter

LSD Least significant difference

MFDM Magnetic Flux Density Meter

MHA Muller-Hinton agar

MM Millimeter

MRSA Methicillin-Resistant Staphylococcus Aureus

NaCl Sodium chloride

PBM Photobiomodulation

PDT Photodynamic Therapy

PPIX Protoporphyrin-IX

PS Photosensitizers

ROS Reactive Oxygen Species

T Tesla

TB Toluidine Blue Dye

UV Ultraviolet

Vis Ultraviolet-Visible

X Xylazine

LIST OF APPENDICES

Appendix A Light Transmission Measurement

Appendix B MRSA Inactivation (In Vitro)

Appendix C MRSA Viability (In Vivo)

Appendix D Instruments Used in the Study

Appendix E Official Approvals

APLIKASI TERAPI FOTODINAMIK DENGAN MEDAN MAGNET DAN PEWARNA UNTUK RAWATAN JANGKITAN KULIT MIKROB SECARA IN VITRO DAN IN VIVO

ABSTRAK

Salah satu kemajuan yang paling ketara dalam menangani isu kulit mikrobial melibatkan pengoptimuman keberkesanan aPDT. Medan magnet (MF) secara meluas digunakan dalam pelbagai aplikasi terapeutik kerana sifat biofizikal mereka yang memberi pengaruh terhadap pelbagai proses biologi. Kajian ini bertujuan untuk meneroka pendekatan pelbagai aspek yang disediakan oleh ciri-ciri ini terhadap mekanisme tindakan aPDT dalam kedua-dua seting in vitro dan in vivo. Pada awalnya, kajian memberi tumpuan kepada menentukan kedalaman penetrasi dan transmisi cahaya laser pada pelbagai panjang gelombang melintasi pelbagai tisu in vitro. Kajian menggunakan model tisu, termasuk daging ayam dan daging lembu dengan ketebalan yang berbeza, untuk memahami kesan panjang gelombang yang berbeza terhadap kesan antimikrob. Pada masa yang sama, PS akan disediakan dari sumber tumbuhan yang berbeza menggunakan kaedah pengekstrakan semulajadi, menyumbang kepada pembangunan aPDT in vivo. Selain penyelidikan ini meneroka impak laser dalam aPDT, ia juga mengkaji pengaktifan Methicillin-resistant Staphylococcus Aureus (MRSA) dalam tisu in vitro sama ada dengan atau tanpa aplikasi MFs luaran. Selanjutnya, penyiasatan melibatkan skenario in vivo, menyelami keberkesanan laser aPDT dengan atau tanpa MFs luaran dalam model tikus dengan luka terinfeksi MRSA. Pendekatan pelbagai aspek ini bertujuan untuk mendalamkan pemahaman aPDT dan mungkin meningkatkan kebolehgunaannya dalam pengaturan klinikal. Pemeriksaan kedalaman penetrasi dan transmisi cahaya laser mendedahkan kedalaman yang berbeza pada panjang gelombang 532 nm dan 660 nm dalam pelbagai jenis tisu in vitro. Dalam penerokaan menyeluruh PS berasal dari tumbuhan untuk tujuan in vivo, senyawa ini menunjukkan sifat unik dan spektrum penyerapan yang berbeza dalam julat panjang gelombang yang digunakan dalam aPDT. Selain itu, in vitro, hasil menunjukkan perbezaan laser yang berbeza dalam aPDT, sama ada dengan atau tanpa aplikasi MFs luaran, berbanding dengan kumpulan kawalan. Ini menekankan impak penting aplikasi laser terhadap pengaktifan MRSA dalam tisu dengan ketebalan yang berbeza. Temuan in vivo menyoroti pengurangan yang signifikan secara statistik (P < 0.05) dalam kelangsungan MRSA di semua kumpulan rawatan berbanding dengan kumpulan kawalan. Secara khusus, aplikasi bersama aPDT dan MFs luaran menunjukkan kesan sinergistik bersama, meningkatkan secara signifikan proses penyembuhan luka pada tikus terinfeksi MRSA pada tahap kepentingan (P = 0.034, P = 0.028) untuk keduadua panjang gelombang 530 nm dan 660 nm selama empat hari berturut-turut. Penyelidikan menekankan impak besar cahaya laser terhadap ketebalan tisu, mendedahkan hubungan rumit antara penetrasi/transmisi dan ketebalan tisu. Pemahaman menyeluruh ini menerangkan bagaimana komposisi tisu mempengaruhi parameter rawatan. Temuan kajian ini memberikan pandangan berharga dalam pembangunan terapi bergerak sasaran untuk jangkitan kulit mikrob, membuka jalan untuk kemajuan potensi dalam aplikasi klinikal aPDT.

APPLICATION OF PHOTODYNAMIC THERAPY WITH MAGNETIC FIELDS AND DYES FOR THE TREATMENT OF MICROBIAL SKIN INFECTIONS IN VITRO AND IN VIVO

ABSTRACT

One of the most notable advancements in addressing microbial skin issues involves optimizing the efficacy of aPDT. Magnetic fields (MFs) are widely employed in diverse therapeutic applications due to their biophysical properties that exert influence over a wide range of biological processes. This study aims to explore the multifaceted approach that these qualities provide to the mechanism of action of aPDT in both in vitro and in vivo settings. Initially, the study focuses on determining the depths of penetration and transmission of laser light at various wavelengths across diverse tissues in vitro. The study used tissue models, including chicken breast and beef of different thicknesses, to comprehensively understand the impact of different wavelengths on antimicrobial effects. Concurrently, PS will be prepared from different plant sources using natural extraction methods, contributing to the development of in vivo aPDT. Additionally, the research explores the impact of lasers in aPDT, examining the inactivation of Methicillin-resistant Staphylococcus Aureus (MRSA) in vitro tissues both with or without the application of external MFs. Furthermore, the investigation extends into in vivo scenarios, delving into the efficacy of laser aPDT with or without external MFs in rat models with MRSAinfected wounds. This multifaceted approach seeks to deepen the understanding of aPDT and potentially enhance its applicability in clinical settings. The examination of penetration and transmission depths of laser light reveals varying depths at wavelengths of 532 nm and 660 nm in diverse tissue types in vitro. In the comprehensive exploration of plant-derived PS for in vivo purposes, these compounds exhibit unique properties and varying absorption spectra within the wavelength range used in aPDT. Moreover, in vitro, results showed variable distinctions in laser utilization within aPDT, both with and without the application of external MFs, compared to control groups. This underscores the significant impact of laser application on MRSA inactivation within tissues of varying thicknesses. The in vivo findings highlight a statistically significant (P < 0.05) reduction in MRSA viability across all treated groups compared to the control group. Notably, the combined application of aPDT and external MFs shows combined synergistic effects, significantly enhancing the wound-healing process in MRSA-infected rats at significance levels (P = 0.034, P = 0.028) for both 530 nm and 660 nm wavelengths over four consecutive days. The research emphasizes the substantial impact of laser light tissue thickness, revealing nuanced relationship between penetration/transmission and tissue thickness. This comprehensive understanding sheds light on how tissue composition intricately influences treatment parameters. The findings of this study provide valuable insights into the development of targeted therapies for microbial skin infections, paving the way for potential advancements in clinical applications of aPDT.

CHAPTER 1

INTRODUCTION

1.1 Background of the Study

Photodynamic Therapy (PDT) is an innovative and promising method that is relatively less invasive and has a different course from other light-stimulating treatments such as photo-thermal therapy (Qiu et al., 2016). This treatment method requires the presence of three main important components: light, oxygen, and some light-absorbing dyes called photosensitizers (PS) to induce a photochemical reaction (Carrera et al., 2016). Light stimulates the PS to produce lethal reactive oxygen species (ROS), such as singlet molecular oxygen ($^{1}O_{2}$), by transferring energy to the ground triplet state of molecular oxygen ($^{3}O_{2}$) (Xia et al., 2014). These ROS exhibit reactivity with lipids, proteins, and DNA (Carrera et al., 2016), leading to cell death by necrosis or apoptosis. PDT, which is characterized by its targeted nature, is proving to be an optimal treatment with minimal impact on the biological system, making it preferred for patients seeking topical therapy (Qiu et al., 2016).

The versatility of PDT extends beyond cancer treatment to various medical applications, including non-cancer fields like ophthalmology, urology, and antimicrobial approaches (Algorri et al., 2021; Krummenauer et al., 2005). It excels in managing precancerous diseases, functional disorders, and microbial skin conditions (Kharkwal et al., 2011). Low-Level Laser Therapy (LLLT), a component of PDT known as photobiomodulation (PBM) (Silva et al., 2015), enhances cellular impact by promoting adenosine triphosphate (ATP) synthesis in mitochondria through exposure to specific light wavelengths (Zahra, 2019). This stimulates cell

proliferation, mitosis in cultured cells, collagen production, and DNA/RNA creation (AlGhamdi et al., 2012; Zahra, 2019).

Despite the successes of PDT, limitations such as redness, swelling, skin sensitivity, and infection hinder improving the patient's overall quality of life (Wang et al., 2020; Wu et al., 2021). This study addresses these challenges and explores innovative approaches synergistic with PDT. External magnetic fields (MFs) are introduced for their potential to influence biological processes, aiding healing and recovery (H. Wang & Zhang, 2017; B. Zhang et al., 2023). These fields modulate cellular activities, impacting ion channels, membrane permeability, and intracellular signaling pathways (Lin, 2012). This modulation contributes to cellular responses crucial for tissue repair, regeneration, and recovery, presenting a promising avenue to enhance PDT results.

The study aims to investigate the effectiveness of LLLT, specifically at wavelengths of 530 nm and 650 nm, in conjunction with PDT for chronic wounds involving bacterial invasion, particularly those caused by Methicillin-Resistant Staphylococcus Aureus (MRSA). The biophysical effects of applying external MFs as a supplement to LLLT in PDT may enhance biological processes and improve light penetration, addressing challenges associated with MRSA infections in vitro and in vivo.

1.2 Problem Statement

Antimicrobial photodynamic therapy (aPDT) is emerging as a promising approach for treating microbial skin infections (Cieplik et al., 2018), using PS activated by specific light wavelengths to produce ROS selectively damaging microbial cells (Dai et al., 2009; Niculescu & Grumezescu, 2021). However, aPDT effectiveness is hampered by light's limited penetration into the skin, impacting microbial inactivation and clinical results (Sperandio et al., 2013). To address this problem, leveraging external magnetic fields (MFs) is proposed to enhance PS delivery (Balhaddad et al., 2021), mitigating damage to host tissues and exhibiting diverse biological effects, including cellular regulation and tissue regeneration (Henry et al., 2008; Zablotskii et al., 2018).

Another strategy involves using natural PS from plants, offering advantages such as enhanced biocompatibility and selectivity against microbial cells (Hochma et al., 2021; Polat & Kang, 2021). Despite promising results, optimizing aPDT for microbial skin infections requires further research, especially in exploring parameters for external MFs. This includes MF types, flux density, target location, penetration depth, exposure time, and sample distance (Markov, 2007). Efficacy comparisons between natural and synthetic PS, like toluidine blue dye (TB), are crucial due to potential synthetic PS toxicity, which may lead to adverse effects on normal tissues (Li et al., 2018).

This study aims to explore the supplemental use of aPDT with external MFs and specific dyes for treating microbial skin infections in vitro and in vivo. In vitro, assessments include laser light penetration and transmission across tissue types, while in vivo development of aPDT with naturally extracted PS from various plant

sources is examined. The impact of lasers in aPDT, with/ without external MFs, to inactivate MRSA is assessed. The study also investigates laser-based aPDT effects, with/ without external MFs, in the in vivo MRSA-infected rat wound models.

The results could significantly impact microbial skin infection treatment, providing more effective therapeutic approaches. Additionally, the study aims to enhance understanding of the biophysical mechanisms involved in combining external MFs with aPDT and to confirm the effectiveness of natural PS in combating microbial infections.

1.3 Research Objectives

The main objective of this study was to investigate the effectiveness of combining aPDT with external MFs and specific dyes as an adjunctive treatment for microbial skin infections in vitro and in vivo, leading to a more effective and comprehensive approach to treating microbial skin infections. To explore the potential synergistic effects of the combined treatment, the specific objectives of the work are summarized in the points below:

- To determine the depths of penetration and transmission of laser light at various wavelengths in different types of tissues in vitro.
- To prepare PS from different types of plants by natural extraction for use in the development of in vivo aPDT.
- iii) To investigate the effect of lasers in aPDT with/without the use of external MFs to inactivate MRSA in the vitro tissue.
- iv) To investigate the effect of laser aPDT with/without the use of external MFs in the in vivo MRSA-infected wound rat models.

1.4 Originality of the Study

This groundbreaking study is the first of its kind to explore the effectiveness of 532 nm and 660 nm of LLLT in combination with aPDT, combined with external MFs stimulation, both in vitro and in vivo. In this work, the effect of lasers in aPDT with/or without the use of external MFs to inactivate MRSA will be investigated, as an indication of maximum light penetration in vitro tissue. In this regard, chicken breast and beef tissues of different thicknesses, including (1, 3, 5, 10, and 20 mm) will be used using a continuous diode laser with a conventional photochromic dye, such as TB dye. The percentage of MRSA viability will be calculated at each thickness. In vivo, the efficacy of the laser will be evaluated in the presence of the natural chlorophyll pigment with/without the use of external MFs for the treatment of wounds of MRSA-infected rats. After treatment, the percentage of MRSA viability is determined and histologically evaluated. However, studying the penetration depth and penetration of laser light in vitro aims to provide detailed knowledge of the most important features that fit the magnetic stimulation parameters based on the limited penetration depth, energy density, and inter-sample distance. This method will provide a novel about the performance of each component of PDT in combination with external MFs both in vitro and in vivo.

1.5 Scope of the Study

The primary aim of this research is to assess the effectiveness of combining aPDT with external MFs, both in vitro and in vivo. The optimization of aPDT effectiveness involves using lasers to measure light penetration depth and transmittance at various wavelengths. The penetration depth is crucial as it correlates with the efficiency of PS in triggering photochemical or photophysical reactions in

cells and microorganisms, considering magnetic stimulation parameters such as penetration depth, flux density, and sample distance. In vitro experiments involve estimating the maximum penetration of 532 nm and 660 nm laser light in laboratory tissues like chicken breast and beef with different thicknesses (1, 3, 5, 10, and 20 mm). The selection of magnetic stimulation parameters is guided by the physical and biological properties obtained from the interaction of laser light with the tissue.

The subsequent investigation focuses on the impact of lasers in the presence of classical PS such as TB in aPDT with/ without the application of external MFs, to inactivate MRSA. This serves as an indicator of maximum light penetration in vitro tissues. Additionally, PS will be derived from various plants through natural extraction, extracted at different durations (4, 8, 12, 16, 20, and 24 hours), and characterized by their physical and chemical properties (pH, density, molecular weight, electrical conductivity, centrifugation, UV-visible spectroscopy, fluorescence, and Fourier transform infrared (FTIR)). The characterization of these dyes aims to validate their use as PS, providing spatiotemporal selectivity to photoluminescence and triggering photochemical or photophysical interactions along with external MFs.

Finally, the research will investigate the in vivo efficacy of the laser in the presence of natural PS with/ without the use of external MFs, using 100 MRSA-infected Wistar rats. The MRSA viability of all irradiated and non-irradiated samples (controlled samples) will be analyzed using SPSS software. Histological evaluations of each treatment group will be performed and compared for comprehensive in vivo research studies.

1.6 Outline of Thesis

This thesis contains five chapters. The first chapter describes the background of this study, problem statement, research objectives, originality, scope of the study, and outline of the thesis. The second chapter reviews the relevant studies and provides the theoretical background for this study and its basic principles. Chapter three explains the tools, materials used in this research study, and methodologies such as experimental arrangement, setup, protocol, and data acquisition. The fourth chapter presents the results, discussion, and data analysis of this research study. The final chapter, chapter five, summarizes the conclusion and provides recommendations for future research endeavors.

CHAPTER 2

LITERATURE REVIEW AND THEORETICAL BACKGROUND

2.1 Introduction

This chapter discusses evidence-based literature reviews on the efficacy of PDT and its core components, such as LLLT and PS, as well as their classes, required criteria, mechanism of action, hypotheses, and therapeutic applications in vitro and in vivo. Publications on the effectiveness and influence of external magnetic and electromagnetic fields will also be considered, as well as the methodologies and standards required to influence different biological systems as they operate in a clinical setting. Finally, advances in studies of external magnetic stimulation when used in combination with lasers in PDT will be described, as well as their promise for treating a range of functional problems, particularly microbial skin diseases.

2.2 Photodynamic therapy (PDT)

Light has been noticed to have healing potential since antiquity (Hamblin & Huang, 2017), with phototherapy being traced back to ~3000 B.C. (Kim et al., 2015). Back then, exposure to sunlight was employed to treat various ailments, ranging from mood and mental health issues to locomotor disorders and skin diseases (Correia et al., 2021; Mitton & Ackroyd, 2008). The discoveries of the infrared spectrum, ultraviolet radiation, and electromagnetic induction, coupled with the invention of artificial light sources, significantly contributed to the emergence of modern phototherapy (Rajesh et al., 2011).

Oscar Raab was the first person to describe the fundamental idea behind photodynamic action in the year 1890. He did so when he observed the toxic effects of acridine orange, which demonstrated activity as a PS when combined with light and oxygen by destroying Paramecium caudatum cells without causing any obvious damage to the protozoa when used alone (Kim et al., 2015). In many experiments, phototherapy has been used for a very long time, especially after many proponents of clinical studies praised this type of treatment when they used a group of PS or so-called hematoporphyrin derivatives (HPD) that react easily to light, which is considered a marker prominent in contemporary light therapy (Rajesh et al., 2011).

It is now known that PDT relies on the PS ability to absorb harmless visible light, which results in the production of ROS in the form of single oxygen ($^{1}O_{2}$), which destroy cancer cells, blood vessels, and dangerous microbes (Kim et al., 2015). Currently, PDT is widely used to treat cancer and many non-cancerous diseases that are defined by excessive growth of unwanted or abnormal cells, as well as foreign cells (viruses, fungi, bacteria) (Dharmaratne et al., 2020). Since then, PDT has undergone continuous evolution, expanding its clinical application beyond the treatment of tumors. Dr. M. Weber recognized as a trailblazer in modern laser therapy, has further employed PDT to address bacterial, viral, and parasitic diseases in a practice known as aPDT (Correia et al., 2021). Furthermore, the most significant help has come from medicinal chemists via the synthesis and finding of new molecules useful for mediating PDT. Some are antimicrobial and some are anticancer, although there are significant variances between them (Abrahamse & Hamblin, 2016; F. Wang et al., 2022).

2.3 Putative mechanisms of action of PDT

Generally, PDT relies on three key elements, such as light, PS, and oxygen to facilitate photosynthesis. When a PS is stimulated by a specific wavelength or light energy, it transitions from the ground state (S_0) to the first excited state (S_1) , leading to the generation of ROS. These species exert various biological effects, including the damage of toxic cells and the stimulation of immune responses (Gunaydin et al., 2021). The excited PS moves across the intersystem boundary from S_0 to S_1 , reaching the long-lived metastable triplet state. From this state, it either transfers energy or hydrogen to the ground state. Through two distinct types of reactions, this active PS can selectively induce cell death by utilizing the generated energy (Rkein & Ozog, 2014).

In a type I reaction, PS can directly engage with a substrate, such as intracellular molecules or components of the cell membrane. This interaction leads to the formation of radicals, which subsequently react with oxygen to produce ROS. Conversely, the second reaction involves the direct transfer of energy from the triple-state PS to the ground-state molecular oxygen (${}^{3}O_{2}$), resulting in the creation of non-radical but highly reactive singlet oxygen (${}^{1}O_{2}$). Notably, this latter process holds greater significance in the context of the current research (Zhu & Finlay, 2008), as further detailed in Figure 2.1.

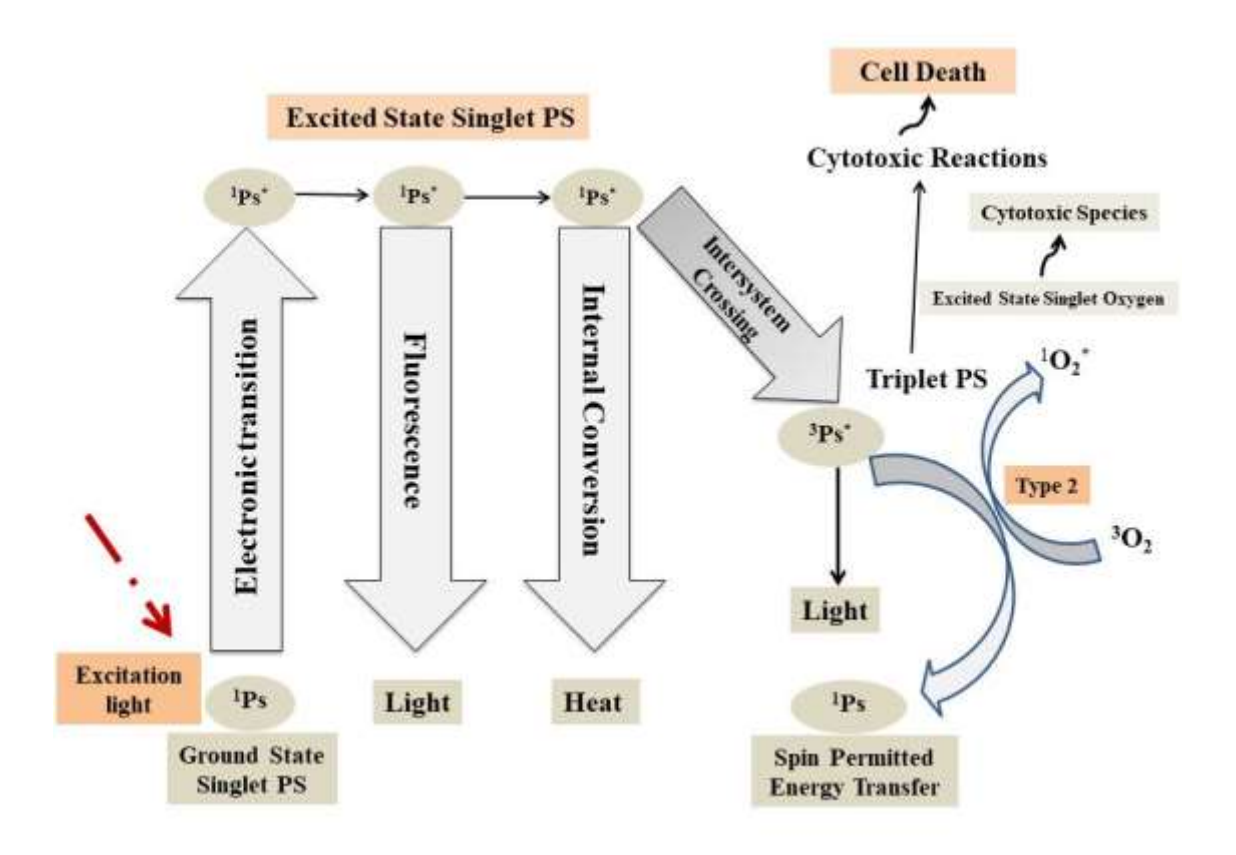


Figure 2.1 A typical scheme of the mechanism of action of PDT (Zhu & Finlay, 2008)

Two approaches have been employed to investigate PDT. The first involves a microscopic model that considers the diffusion of oxygen and PS from blood vessels, enabling the microscopic determination of ${}^{1}\text{O}_{2}$ concentration within cells. Foster et al. pioneered this quantitative model, validating its results using multicellular tumor spheroids. These models highlight that the primary influence on the efficacy of photodynamic treatment is largely associated with the rate of oxygen consumption during the photochemical process (Bulin & Hasan, 2022; Zhu & Finlay, 2008). PDT can induce transient hypoxia if the rate of photochemical oxygen consumption surpasses the rate at which oxygen can be replenished by the vasculature or ambient media. This phenomenon, theoretically hypothesized and observed in animal and human tissues, remains an active area of research (Penjweini & Zhu, 2015; Zhu & Finlay, 2008).

Additionally, the synthesis of ${}^{1}O_{2}$ was initially believed to be dependent on the oxygen content in living tissues. When cells experience significant oxygen deprivation, the photodynamic machinery may detect photosensitivity at a rate that contributes to the generation of transient hypoxia, inhibiting subsequent photosensitizing effects. Conversely, hyperbaric oxygenation has been demonstrated to enhance the photosensitizing effect, contingent on the efficiency of the PS, the rate of light fluorescence, and the distribution of medium oxygenation in tissues (Allison & Moghissi, 2013; Penjweini & Zhu, 2015).

2.4 Putative mechanisms of action of aPDT

Based on the combination of a non-toxic PS and a specific wavelength of visible light, aPDT can generate a phototoxic reaction when triggered in the presence of ambient oxygen. The created ROS have the ability to damage biomolecules and oxidize cellular components, by adjusting the light dose (fluence) and wavelength to optimize the activation of the PS. This helps in regulating the amount of ROS produced and the depth of penetration into tissues, which results in the death of microorganisms (Dharmaratne et al., 2020; Ran et al., 2021). Each of these elements light, PS, and oxygen is safe by itself, but when they come together, they may create deadly cytotoxic ROS that can kill cells on purpose (Dharmaratne et al., 2020). The mechanism of action of aPDT can be briefly explained as follows: it involves the excitation of a non-toxic, light-absorbing dye to create a long-lasting triple excited state that transfers energy to nearby molecules, usually into $^{1}O_{2}$, to produce highly cytotoxic ROS such as hydroxyl radicals (Figure 2.2). ROS can damage DNA or even the structure of the plasma membrane and promote microbial cell death through a variety of mechanisms, including lipid peroxidation, inhibition of enzymatic

systems, and accumulation of proteins required for other biological systems (Diogo et al., 2019; Youf et al., 2021).

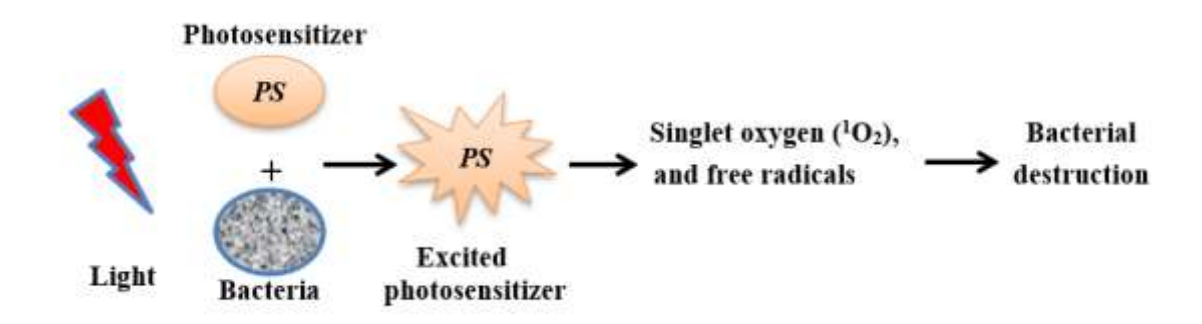


Figure 2.2 Scheme of the mechanism of activation of aPDT (Carrera et al., 2016)

2.5 PDT Components

2.5.1 Photosensitizers

The majority of photosensitizers used in PDT in the middle of the 20th century were derived from hematoporphyrin (HpD) or so-called (Photofrin), an endogenous porphyrin produced in the initial phase of the biosynthesis of heme. Heme is an iron-containing molecule that is a crucial component of hemoglobin, myoglobin, and various enzymes. The endogenous porphyrin derived from heme, such as HpD, can result in severe phototoxicity and persistent, strong photosensitivity. This is because the photosensitization process requires significant levels of HpD (Abrahamse & Hamblin, 2016). The initial development of photosensitive topical sensitizer, 5-aminolevulinic acid (ALA), marked a significant milestone. A pioneering study employing ALA-mediated PDT demonstrated its efficacy in 11 patients with oral leukoplakia during the first phase. Notably, a safe and effective dose of ALA-PDT was established at a mild 4J/cm², setting a standard for photomedicine practitioners of that era (Kou et al., 2017). At the moment, second-generation sensitizers based on the structure of protoporphyrin IX (PPIX) and

other second-generation sensitizers based on the structure of photosensitizing intermediate porphyrins are the most commonly used precursors. However, research has shown that PPIX has a longer wavelength in red blood cells (RBCs). It is a precursor of heme and is involved in the metabolism of heme through a mix of mitochondrial transport proteins. It can treat multiple lesions at the same time, is not very invasive, is well tolerated, and has a great cosmetic effect (Abrahamse & Hamblin, 2016; Kou et al., 2017). Nevertheless, despite their widespread use, firstgeneration PS have a number of drawbacks. These PS have limited chemical purity and can only be triggered efficiently at wavelengths below 640 nm, limiting tissue penetration. Furthermore, the lengthy half-life of PS makes the skin photosensitive for many weeks, necessitating patients treated with them to stay in a dark room for up to 6 weeks (Kwiatkowski et al., 2018; Park et al., 2018). Therefore, research on the next generation of PS began in the late 1980s. Pure synthesized large-cycle compounds constitute second-generation PS aromatic (e.g., porphyrins, benzoporphyrins, chlorines, bacterial chlorines, and phthalocyanines) (Niculescu & Grumezescu, 2021). Contrarily, some first- and second-generation sensitizers had low water solubility, light penetration depth, and tumour targeting efficacy, which reduced ROS production (Chhablani, 2010; Pérez-Pérez et al., 2014). Considering the simplicity with which PS and light may be administered into the skin, it is not unexpected that innovative PDT-supportive therapy modalities are increasingly being employed to accelerate advanced biological responses to cure diverse illnesses caused by bacteria, fungi, and viruses.

2.5.2 Toluidine blue dye (TB)-Induced Protoporphyrin IX (PPIX)

TB, also called tolonium chloride, is a metachromatic acidophilic dye that stains only acidic parts of tissue (sulfates, carboxylates, and phosphate radicals). TB has a strong attraction to nucleic acids, so it sticks to the nuclei of tissues with a lot of DNA and RNA (Sridharan & Shankar, 2012). This dye appears basic as substrates with accessible anionic radicals and has solubility in both water and ethanol. Despite being a staining method that has been around for a very long time, it is widely used in modern biological research. The Web of Science research network cited over 4800 publications addressing TB usage in November 2018. These articles totaled 245 and were released in 2018 (de Campos Vidal & Mello, 2019).

TB was utilized as an adjuvant to an antimicrobial photodynamic chemotherapeutic experiment to reduce the viability of biofilms generated by bacteria and fungus. TB absorbs the most light with orthogonal tissues at large range of 600–660 nm, resulting in a blue staining. Regarding color change, the absorption spectrum is red and peaks between 480 and 540 nanometers (de Campos Vidal & Mello, 2019; Jajarm et al., 2015). Despite the fact that TB has a high potential for destroying microorganism cell membranes through the creation of radical forms of ROS, it has recently been proven to be widely employed in clinical research as a PS for aPDT (Suvorov et al., 2021).

2.5.2(a) Natural chlorophylls

Currently, a new pigment found in plants, algae and bacteria called chlorophyll is being studied extensively. Chlorophyll's absorption spectrum spans 400 to 700 nm, with two absorption maxima at 415 and 630-664 nm. When compared to synthetic analogs, chlorophyll has the benefit of being less expensive,

having a shorter incubation period, and being able to serve as a PS in less time. Chlorophyll could be a crucial component of an effective alternative therapy for individuals with bacterial and malignant disorders (Kim et al., 2015; Kustov et al., 2018). This Chlorophyll dye is used as a sensitizer in PDT because it traps light energy, enhances cellular uptake, and produces high ROS upon light irradiation (Suvorov et al., 2021). Also, Chlorophyll-enriched plant extracts have positive photodynamic effects because they have a high quantum yield of ${}^{1}O_{2}$ and a high absorption of visible light (Polat & Kang, 2021). However, due to the aforementioned properties, tests revealed that chlorophyll has high antimicrobial activity under irradiation in aPDT via complete inactivation of bacterial cells, whereas no cytotoxic effects were observed in a similar experiment with healthy cells (Kustov et al., 2018; Suvorov et al., 2021).

2.5.3 Light source, transport, and delivery

Optimal selection of a light source for PDT requires careful consideration of the most effective PS. Choosing a light with a wavelength that aligns with the peak activation spectrum of porphyrins in tissues is crucial to achieving the maximum therapeutic impact of PDT (Kim et al., 2015). The required depth of penetration dictates the light source used in PDT. The visible and near-infrared spectra allow for deeper penetration. When working with porphyrin sensitizers, blue light in the band (410 nm) is more effective than red light down to 2 mm because of the sensitizers' high extinction coefficient in the blue area (Hathaway & Sliney, 2016). The extinction coefficient specifically refers to the ability of a substance to absorb light at a particular wavelength, indicating how effectively it absorbs or attenuates light at that specific wavelength. The selected PS absorption spectra must match the

specified wavelength (Mitton & Ackroyd, 2008). Based on this, the photodynamic efficacy of various surface and interstitial treatment locations may be modified by adjusting the optical penetration depth of the excitation light, the wavelength, the effect, and the time interval of drug light using guest-band laser light sources (Algorri et al., 2021).

Lasers have been studied for many years to see if they can be used to treat cell cultures. Belkin and Schwartz found that this kind of light changes the way cations and anions, especially calcium, move through membranes in a big way. The way a laser and tissue interact is photochemical, and it depends on how light is absorbed by a chromophores in the tissue, such as an enzyme, a molecule in a membrane, or another cellular or extracellular part. The absorption makes the chromophores more energetic and causes molecular reactions that change biochemical pathways. As a result, the cell's metabolism is changed, which affects tissues and organs (Carrera et al., 2016).

2.5.4 Tissue oxygen

The PDT induces cytotoxic mediators, which in turn need endogenous ground-state 3O_2 in the tissue, while the photodynamic effect requires exogenous PS and light dose. The efficiency of the PS process is proportional to the amount of 1O_2 produced in the tumor microenvironment, which is the most reactive oxygen form species causing PDT cytotoxicity. The production of 1O_2 is also dependent on the oxygen level in the body's tissues. Hypoxic cells are extraordinarily resistant to PS because the photodynamic response mechanism may use oxygen at a rate sufficient to establish a situation of transitory hypoxia and inhibit future PS effects (Henderson & Gollnick, 2014).

2.6 Tissue regeneration and wound-healing

Wound healing is a dynamic mechanism associated with several events that include bleeding, coagulation, early inflammatory response, regeneration, migration, and proliferation of connective tissue and parenchyma cells, as well as the formation and reorganization of extracellular matrix (ECM) proteins (Gonzalez et al., 2016). The onset of hemorrhage into the wound site and the subsequent activation of the clotting cascade mark the start of the mending process. Clotted blood functions as a matrix that controls cell adhesion and movement. Platelets play a key role in wound healing by supplying inflammatory cells and fibroblasts with growth factors and proinflammatory cytokines (Tsala et al., 2013). Neutrophils and macrophages fight invading germs while also supporting the healing process by producing a variety of cytokines and growth factors that trigger the granulation tissue development phase. This tissue is made up of endothelial cells, macrophages, fibroblasts, and a new extracellular matrix and serves to cover and heal the wound (Gonzalez et al., 2016). Cell adhesion, motility, and proliferation are aided by the components of the temporary extracellular wound matrix. Following keratinocyte growth and migration at the wound edge, re-epithelialization restores tissue integrity (Rousselle et al., 2019). Lastly, during remodeling, granulation tissue retraction and transformation into scar tissue depend on the balance between scar matrix component creation and protease destruction. These processes include vascular regression, fibroblast differentiation into myofibroblasts, replacement of the temporary ECM with a permanent collagenous matrix, and most importantly, inflammatory response resolution (Singh et al., 2017).

Moreover, wounds are classified as acute or chronic based on how long they take to heal (Krzyszczyk et al., 2018). Acute wounds mend and heal spontaneously

over the period of two to three weeks from the time of damage and may take months or longer to complete. Chronic non-healing wounds occur when wounds do not heal in a timely and organized manner (ulcers). These wounds are ones that have not made it through the typical stages of healing and are marked by chronicity as well as repeated relapses (Harper et al., 2014; Singh et al., 2017).

2.7 Light Technology for Topical PDT

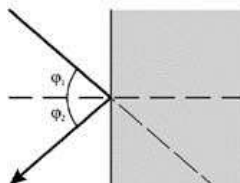
2.7.1 Light interaction with biological tissue

The interaction of light with biological tissues is very important in PDT, as it follows the management of PS activation by visible or infrared light at a specific wavelength (Algorri et al., 2021; Alva-Sánchez et al., 2021). Photons that pass through tissues undergo many physical processes such as absorption, reflection, refraction, dispersion, and fluorescence, as illustrated in Figure 2.2.

a - Refraction **b**-Reflection

 Minimized by perpendicular light application

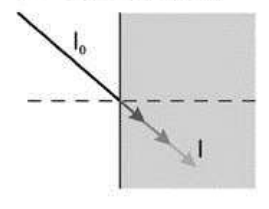
Snell's Law n,



· Minimized by perpendicular light application

Fresnel's Law $\varphi_1 = \varphi_2$

C - Absorption



- · Depending on tissue composition
- · Determining the optical window for PDT (see Figure 2)
- · Minimized by activation in the far-red wavelengh region

Lambert-Beer's Law

$$I_x = I_0 e^{-\alpha_{abs} *_X}$$

d - Scattering

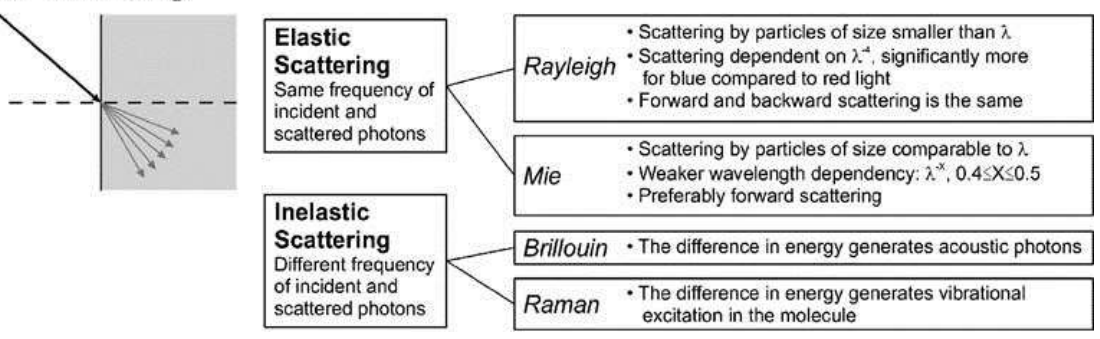


Figure 2.3 Interactions between light and tissue (Plaetzer et al., 2009)

In general, these physical properties can be described, and their effect on tissues determined as follows:

2.7.1(a) **Absorption**

Lambert-Beer's law states that absorption occurs when a photon possesses energy that aligns with the energy gap between two molecular levels. This phenomenon is primarily attributed to the presence of internal tissue chromophores, including hemoglobin, myoglobin, melanin, and cytochrome. These chromophores define a "windowed tissue" where light can deeply penetrate, and the wavelength range spans from 630 to 1300 nm (Mäntele & Deniz, 2017). In the context of light transmission measurement in PDT, this law could be applied to describe how the concentration of the PS in the tissue or solution affects the absorption of light (Carrera et al., 2016), this process can be described as follows:

$$I_{transmitted} = I_{incident} \cdot T \cdot 10^{-A}$$
 (2.1)

where $I_{transmitted}$ is the intensity of transmitted light, $I_{incident}$ is the incident light intensity, T is the transmission coefficient, and A is the absorbance.

2.7.1(b) Reflection

According to Fresnel's law, reflectance denotes the fraction of incident light that rebounds from the tissue surface without being absorbed or internally scattered. Essentially, it quantifies the light that reflects or bounces off the tissue surface (Keiser & Keiser, 2016). The interaction between light and tissue is crucial in PDT for activating photosensitizing agents. When light is directed onto the tissue surface, processes like absorption, scattering, and reflection may take place. Reflectance becomes a pivotal factor in determining the extent to which light penetrates the tissue, reaching specific depths where PS are located (Algorri et al., 2021). Notably, Fresnel's Law addresses the reflection and transmission of light at interfaces with different refractive indices, offering insights into how light behaves during its passage through the tissue. When considering light transmission through a medium, the transmission coefficient (T) becomes a key parameter of interest.

$$T = 1 - R \tag{2.2}$$

where R is the reflection coefficient. The reflection and transmission coefficients depend on the angle of incidence, the refractive indices of the media, and the polarization of light.

2.7.1(c) Refraction

According to Snell's law, there is a visual phenomenon, which is observed when the photon beam penetrates the tissues that change direction. Refraction in the context of PDT refers to the bending of light as it passes through the tissue surface into deeper layers (Algorri et al., 2021; Keiser & Keiser, 2016). This phenomenon occurs because the speed of light changes as it transitions from one medium (such as air or a transparent medium) to another (such as biological tissue) with a different refractive index.

In the context of PDT, where light is used to activate photosensitizing agents within tissues, understanding refraction is crucial. The degree of refraction depends on the angle at which the light strikes the tissue surface and the refractive indices of the two media involved (Piksa et al., 2023). The change in the direction of light due to refraction affects the path that light takes through the tissue.

Researchers and clinicians take into account the refractive properties of tissues to optimize the delivery of light during PDT. Proper consideration of refraction helps ensure that the light reaches the target depth within the tissue where the PS are located, contributing to the effectiveness of the PDT.

2.7.1(d) Scattering

Optical phenomenon, defined by Rayleigh-Guns theory, occurs when a photon beam penetrating the tissue is spread in multiple beams with different directions defined by the anisotropy factor. This anisotropy coefficient is an important measure, as its value dictates the degree of broadening that the incident beam will undergo as it travels through the tissues; this in turn, therefore, helps determine the depth of penetration (Jacques, 2013).

2.7.2 Putative mechanisms of action of aPDT upon absorption

Only competing photochemical and photophysical processes that provide a general and simple explanation for the $^{1}O_{2}$ generation of PDT will be covered. These features may reveal the opposing mechanisms and energy transfer processes that influence the effects of the cell death pathway, as reported as follows:

2.7.2(a) Photochemical

In the realm of photochemistry, each PS possesses the capability, under specific conditions, to generate ROS as depicted in Figure 2.1. Typically, a PS resides in a stable electronic configuration referred to as the ground state. Upon exposure to and absorption of a photon, the PS undergoes a transition from a low-energy level (fundamental) state (¹PS) to an excited singlet state (¹PS*) known for its remarkable reactivity but brief duration, termed a "Frank Condon" (Youf et al., 2021). Subsequently, the stimulated particles' singlet ground state absorbs adequate light energy (wavelength) to elevate an electron to a high-energy state.

Upon light absorption by tissue, particles either release heat or emit internal light. The PS-sensitive molecule engages in a fluorescence process, initiating the

formation of a stable state referred to as the "system junction." Here, the excited molecule decays, producing a fluorescent photon and extending the life of the oxygen triplet state (${}^{3}O_{2}$) to microseconds, while reverting to the ground-excited ${}^{1}O_{2}$ in nanoseconds. Due to this temporal difference, the triplet ground state may collide with an oxygen molecule, transferring its energy to form ${}^{1}O_{2}$, which promptly reacts with cells (Comeau et al., 2022).

Additionally, two simultaneous chemical reaction pathways type I electron transfer and type II energy transfer can occur, leading to the generation of ROS. This rapid oxidative burst, as mentioned earlier, is instrumental in bacterial eradication (Cieplik et al., 2017). However, Núñez et al., (2014) study on the influence of ionic strength on the antimicrobial photodynamic efficiency of methylene blue has been commended for revealing potential contradictions in the photochemical reaction mechanism. This stems from microorganisms exhibiting diverse responses to $^{1}O_{2}$ formation and the occurrence of ROS formation in distinct microbial targets, contingent on the type of PS used.

2.7.2(b) Photophysical

The photophysical aspect is a crucial parameter that enhances the effective activation of the 3O_2 , facilitating the excitation of PS with the appropriate wavelength of light. Optimal tissue penetration for 1O_2 generation occurs within the wavelength range of 650 to 850 nm. This efficiency in generating the 3O_2 not only contributes to long-term cases but also plays a pivotal role in tumor localization, the production of toxic byproducts, and the repair of damaged tissues. This underscores the need for continuous research and enhancement of PS to exhibit greater efficacy. Consequently, PS are employed to evaluate variations pre- and post-radiation, as well